JOURNAL OF OPTOELECTRONICS AND ADVANCED MATERIALS Vol. 8, No. 3, June 2006, p. 901 - 908

Improving the wetting of oxides by metals

J. JUPILLE*, R. LAZZARI
Institut des Nanosciences de Paris (INSP), Universités Paris 6 et 7, UMR CNRS 7588, Campus de Boucicaut, 75015 PARIS

On wide band gap oxides, metal atoms show a tendency to cluster in 3D particles. Since this appears to be unfavourable in many advanced technologies which involve metal/oxide interfaces, improving the wetting at these interfaces is a constant challenge. The present paper focuses on some important means that are stressed to strengthen the interfacial bonding, namely the hydroxylation of the oxide surfaces and the pre-deposition of a buffer. The analysis combines the examination of the interfacial metal/oxide chemistry by photoemission and the characterization of the wetting by UV-visible surface differential reflectivity. This technique is shown to be very appropriate for the *in situ* study of growing films.

(Received March 15, 2006; accepted May 18, 2006)

Keywords: Interface metal/oxide, Wetting, X-ray photoemission spectroscopy, Surface differential reflectivity

1. Introduction

There is a considerable interest in the wetting at metal/oxide interfaces. As a test bed for the contact between dissimilar materials, the issue has a great scientific significance because it uncovers a variety of cases, ranging from abrupt to reactive interfaces, from nucleation at random to nucleation on defects, from growth driven by thermodynamics to growth dictated by kinetics. Also strongly exciting are the many applications involving metal/oxide interfaces such as microelectronics (integrated microcircuits, magneto-resistive random access memory), glass industry (low-emissive and anti-solar coatings on glazings), heterogeneous catalysis, high temperature metallurgy, thermal barriers, corrosion protection [1-3].

Most metals poorly wet wide band gap oxides and cluster in three-dimensional (3D) particles when deposited on these substrates. Because it is often found unfavourable, this tendency has challenged various approaches to run counter the natural behaviour by strengthening the bonding at the metal/oxide interface, in particular via either hydroxylation of the oxide [4,5] or pre-deposition of a metallic buffer [6]. After a short review of the trends in wetting at the M/O interfaces, the above issues are discussed through the study of silver, titanium, aluminium, palladium, and silver/titanium thin films deposited on MgO(100) and α-Al_2O_3(0001) surfaces.

In analysis of growing films, *in situ* characterization of the adhesion and/or wetting is of major interest. In the series of experiments reported herein, the hint is to tackle this methodological problem via the modelling of the surface differential UV-visible reflectance which is expected to be very flexible [7,8].

2. Trends in metal-oxide wetting

2.1. General trends

In the limit of a noble metal at the contact of a wide band gap oxide, it is often assumed that the adhesion energy $W_A = W_{bonding} + W_{image} + W_{vdW}$ is dominated by long-range interactions, image (W_{image}) [9] and van der Waals (W_{vdW}) [10] forces, whereas short-range ionocovalent bonding ($W_{bonding}$) is expected to become marginal. A comprehensive theoretical model that could account for all contributions simultaneously is still lacking. Possible reasons are the specific hindrances encountered by calculations involving insulating solids. In particular, the modelling of those poorly screened media requires a large number of atoms to account for the Madelung field and the difficulties in describing electron correlations in insulators have not yet been completely overcome.

In this context, a simple approach [11] consists in modeling the interaction between the two media via a representation of the solid state by a dielectric continuum developed by Barrera and Duke [12], which leads in fact to an estimate of the van der Waals contribution to the overall interaction (Fig. 1). The dielectric continuum model overestimates the surface energy γ_M of the metal and the M/O interface energy γ_{MO}. However, the Dupré expression of the adhesion energy $W_A = \gamma_O + \gamma_M - \gamma_{MO}$ contains the difference $\gamma_M - \gamma_{MO}$ that allows the two terms to partly compensate [11]. When rescaled by a factor 0.5, the estimates of the van der Waals contributions to the adhesion energy W_A of different metals deposited onto silica are in good agreement with the overall values of the adhesion energy deduced from sessile drop measurements [13]. Similar agreement is observed for metals on alumina and metals on glass [11,14]. In the latter case, the overall values of the adhesion energy are deduced from scratch test measurements.

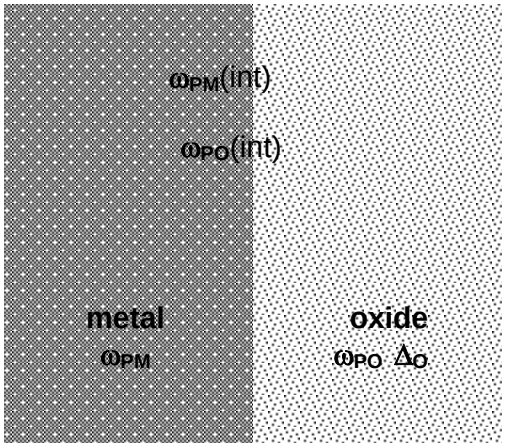

Fig. 1. Schematic representation of the contact between a metal (M) and an oxide (O); the bulk plasmon (ω_p) and transverse mode (Δ), the surface modes (ω_p) and the interface modes ($\omega_{\boldsymbol{p}}^{(\mathrm{int})}$) are indicated (from Ref. 15).

The dielectric continuum model reveals two main trends [11,14,15]. The metal/oxide adhesion increases when the plasmon energy (or the conduction electron density) of the metal increases (the example of metals on silica is given in Fig. 2) and/or when the band gap of the oxide narrows. The prediction is in full agreement with the experimental observations [16].

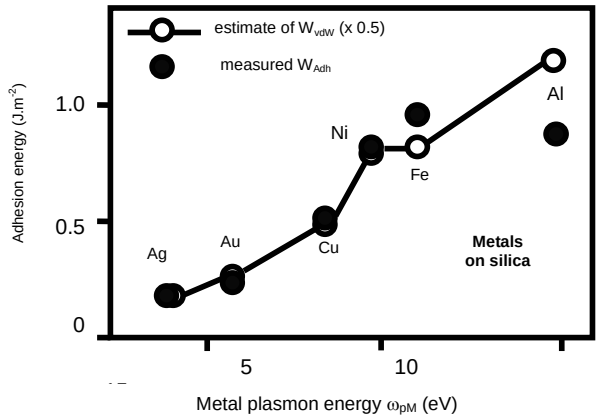

Fig. 2. Trends in adhesion energy at M/O interfaces: comparison between calculated estimates of the van der Waals contribution to the work of adhesion rescaled by a factor 0.5 (W_{vdW}) and values of the overall W_{Adh} deduced from contact angle measurements by the sessile drop method [13] for different metals deposited onto silica (from Ref. 15).

On the contrary, the other type of long-range interactions, due to image forces, does not show a similar trend [15]. This indicates that the van der Waals contribution to the overall adhesion energy is not negligible, at least for metals with low conduction density on wide band gap oxides, in which case the short-range ionocovalent bonding is expected to be marginal. Indeed, it was shown that up to 30 % of the adhesion energy of tungsten on oxide surfaces can originate from van der Waals interactions [17]. This legitimates the above qualitative approach of two media in contact by means of the dielectric continuum formalism.

2.2 Growth modes

The growth modes of a vapour that condenses on a solid substrate are commonly classified into three categories. The so-called Franck-van der Merwe, Stranski-Krastanov and Volmer-Weber growth modes correspond to perfect wetting, wetting of a few layers followed by the emergence of three-dimensional clusters and formation of 3D clusters from the beginning, respectively (Fig. 3) (Ref. 18 and refs. Therein). These growth modes are also defined by different wetting conditions, which are easily understood in the framework of the Young-Dupré expressions of the energy of adhesion $W_{adh} = \gamma_A + \gamma_B - \gamma_{AB} = \gamma_A (1 + \cos\theta)$ of a film A on a substrate B, where θ is the contact angle of A on B. The Stranski-Krastanov growth mode implies that the adhesion energy of the film is strong enough to allow a 2D growth mode of the very first atomic layers at the contact of the substrate while an elastic relaxation occurs on further deposition.

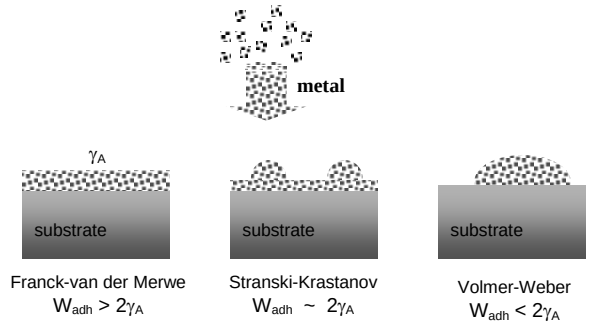

Fig. 3. The common classification of the growth modes of thin films that condense from a vapour on a solid substrate.

The measurement of the contact angle of liquid metals on wide band gap oxides by the sessile drop method demonstrates that the metal/oxide growth mode at equilibrium is always of the Volmer-Weber type (3D) [13,19]. Consistently, most metal/oxide systems studied in vacuum conditions show Stranski-Krastanov or Volmer-Weber growth modes, while the occurrence of apparent two-dimensional growth is generally attributed to kinetic effects [1]. In practice, a distinction may be made between contact angles higher than 90° ($W_{adh} < \gamma_A$) and contact angles lower than 90° ($W_{adh} > \gamma_A$). In the latter case, percolation may occur quickly upon increasing coverage, in particular when kinetics favours the growth of a metastable film. Such behaviour is illustrated by the example of Ti/α-Al_2O_3(0001) which is discussed in Section 3.2.

2.3 Particle shape and growth modes at a glance

The analysis of the liquid metal/solid oxide is a dedicated method to derive thermodynamic parameters. The thorough study of the wetting (adhesion) at growing solid/solid interfaces is not such a clear cut. It requires experimental methods of analysis that can be run *in situ* and during the growth. Grazing incidence small angles x-ray scattering (GISAXS) and surface differential reflectance (SDR) spectroscopy are two such methods. Their capability to define mean particles over numbers of clusters is illustrated in the case of the direct observation of the 3D growth of Pd/MgO(100) (GISAXS) [20] and Ag/α-Al_2O_3(0001) (SDR) [21].

The poor wetting of a cold window by water droplets that condense in a humid atmosphere gives rise to the so-called breath figures [22]. It was anticipated that solid films could grow in a similar way [22], though the nanometer size of the particles could prevent analysis. The analysis of the GISAXS patterns recorded during the deposition of palladium on MgO(100) at 650 K (Fig. 4) [20] demonstrates that the particles are in the form of truncated cuboctaedra. The shape of which can be associated to an adhesion energy of 1.12 $J.m^{-2}$ by means of the Wulff construction, in good agreement with a value of 0.95 $J.m^{-2}$ derived from sessile drop measurements. Moreover, the particles diameter is shown to be about proportional to the average film thickness t during the growth stage and to obey a ~ $t^{0.75}$ law when particles coalesce, in agreement with the parameters observed in breath figures [22].

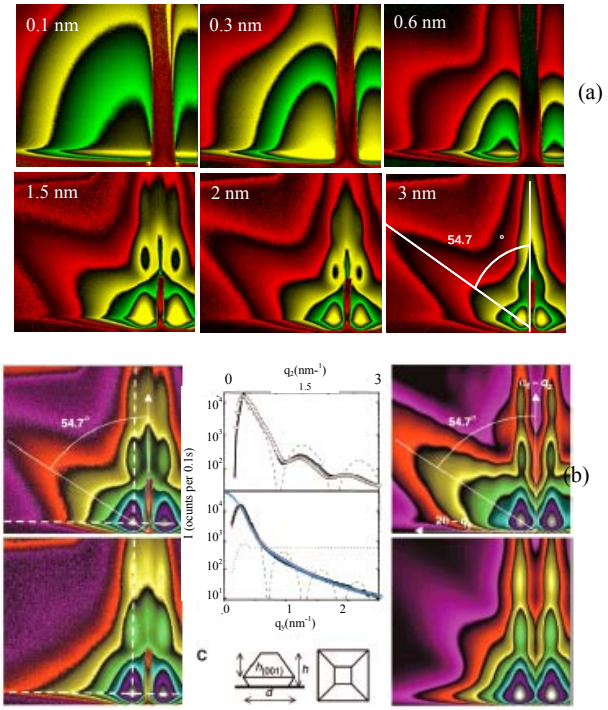

Fig. 4. Growth of palladium on MgO(100) at 650 K by GISAXS (from Ref. 20): (a) GISAXS patterns recorded at various average thicknesses; (b) models of pattern that are consistent with palladium particles in form of truncated cuboctaedra; the feature that shows up at 54.7° with respect to the normal to the surface corresponds to the emergence of (111) facets.

Surface differential reflectance (SDR) of UV-visible light can be also used to analyse a growing film. The principle of the method is schematized in Fig. 5. The SDR spectra are then fitted to models which parameters are the size, aspect ratio and density of either truncated spheres or truncated spheroids [7,8,21]. The more accurate SDR results are obtained in the case of silver films. For example, from the shape of the truncated sphere used to fit the SDR spectrum shown in Fig. 5, the contact angle of silver on α-Al_2O_3(0001) at 573 K was estimated to 125°, in perfect agreement with the sessile drop value of 127°-130° [19] (Table 1). More generally, it was shown that SDR data for silver well compare with GISAXS data [23]. However, the technique also applies to simple metals and transition metals. It is extensively used in the following sections to study the growth of titanium, aluminium and silver films.

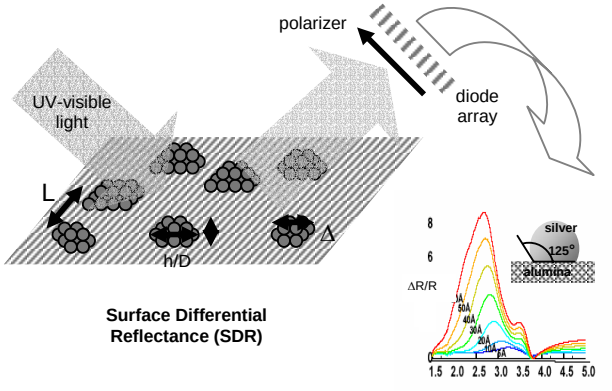

Fig. 5. Schematic representation of the analysis by surface differential reflectance (SDR). The reflected UV-light signal is collected and analyzed after subtraction to a signal taken as an origin. A series of spectra recorded during the deposition of silver on α-Al_2O_3(0001) at 573 K is presented as an example. The model cluster (in the form of a truncated sphere [7]) that allows the best fit is schematized; the derived estimate of the contact angle (125°) is shown (from Ref. 21).

3. Can hydroxylation improve the wetting of an oxide by a metal?

The α-Al_2O_3(0001) surface is very appropriate to test the effects of hydroxylation on the wetting of metal films. As demonstrated both by experiment [24] and theory [25], α-Al_2O_3(0001) dissociatively adsorbs water molecules to give rise to a hydroxylated surface. The deposition of a metal on a hydroxylated alumina surface might be a way to produce the very strong metal/O-terminated alumina bonds, provided that metal can react with hydroxyl groups to give rise to metal-oxygen bonds and release hydrogen. Indeed, the transition metals of the beginning of the series [X] and aluminium [X] are expected to react in such manner with hydroxyl groups (see Ref. 25 and refs. therein). The present work analyses the interfacial chemistry of aluminium and titanium with hydroxylated

alumina surfaces and examines the extent in which the resulting metal-oxygen bonds improve the wetting of the oxide by the metal [4, 5]. About the growth mode of the film, the hint of the present work is to analyse the metallic film during its growth by SDR measurements to directly determine the wetting parameters.

3.1 Chemistry at aluminium/ and titanium/ α-Al_2O_3(0001) interface

The x-ray photoemission spectroscopy (XPS) component that shows up on the higher binding energy side of the O 1s core-level spectra of the bare α-Al_2O_3(0001) surface (Fig. 6a) stems from the presence of hydroxyl groups [26]. At the beginning of the deposition of metallic aluminium, this O 1s component decreases in intensity and finally vanishes, which indicates that it is shifted toward the energy position of the bulk O 1s component (Fig. 6a). The examination of the Al 2s spectra reveals that the deposited aluminium appears in a metallic form only around an average Al film thickness of 2Å (Fig. 6b). Therefore, up to that coverage, the Al 2s component associated with the deposited aluminium film is not distinguishable from the Al 2s component due to the alumina substrate. This and the observation made on the high energy O 1s component is consistent with the prediction by Siegel et al. that aluminium atoms deposited on O-terminated α-Al_2O_3(0001) bonds to oxygen to produce an extra alumina layer prior to forming a metallic aluminium film [27]. The adhesion of the first aluminium atomic layer on the O-terminated (hydroxylated) α-Al_2O_3(0001) surface is expected to be close to 10 $J.m^{-2}$, a very strong adhesion energy value reminiscent of the cohesion energy of the oxide [27].

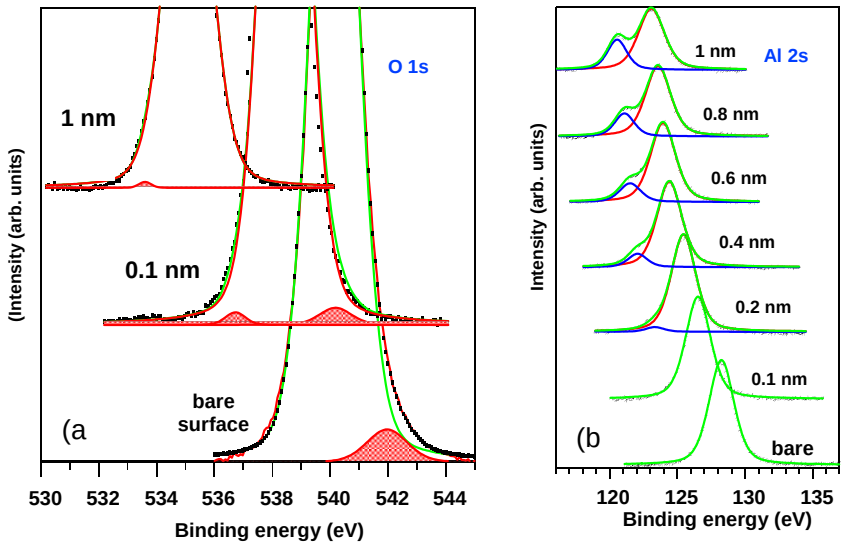

Fig. 6. Photoemission (XPS) recorded during the deposition of aluminium on α-Al_2O_3(0001) : (a) O 1s spectra: the high binding energy component associated with surface hydroxyl groups is shifted toward the bulk O 1s at the very beginning of the deposition; (b) Al 2s spectra: the component associated with metallic aluminium shows up on the lower binding energy side after the deposition of ~ 0.2 nm of aluminium (from Ref. 26).

When titanium is deposited on hydroxylated α-Al_2O_3(0001), photoemission analysis [26] leads to similar conclusion. The very first titanium layer growing at the contact of the hydroxylated alumina is oxidized via a reaction with surface hydroxyl groups. Photoemission analysis identifies Ti^{4+} and Ti^{2+}. Then, titanium remains metallic. Upon the reaction of hydroxyl groups with titanium, the high energy component of the O 1s spectrum is shifted by –2.8 eV toward the low binding energy side of O 1s. Such shift is not at all due to screening since the adsorption of silver on hydroxylated α-Al_2O_3(0001) does not affect the binding energy of the O 1s component assigned to hydroxyl groups. The absence of any shift in the Al 2p spectrum [28] demonstrates that titanium oxides are formed via a surface reaction that does not involve at all the alumina substrate and which can be schematized as Ti + OH -> Titanium oxides + hydrogen. In passing, this examination of the O 1s spectra upon titanium deposition allows the assignment to residual OH groups [26] of the high binding energy O 1s component that is observed even on the clean α-Al_2O_3(0001) surface [24,26].

3.2 Analysis of the wetting by the surface differential reflectivity

SDR spectra recorded *in situ* during the growth of the aluminium film on α-Al_2O_3(0001) at 200 K are shown in Fig. 7a. The position in energy of the resonance (~ 2.5 eV) is indicative of the formation of clusters with very high aspect ratio (diameter/height) since the Frölich mode of aluminium spheres is observed around 9 eV. The occurrence of resonances at the beginning of the growth of the film (Fig. 7b) demonstrates that the very first atoms of aluminium deposited in a metallic form do give rise to

clusters with a similar shape. The aspect ratio of clusters grown at 200 K is estimated to 9 (Fig. 7b) via a truncated sphere model [7]. However, the cluster shape at 200 K is dictated by kinetic effects since, upon deposition of aluminium at 650 K (Fig. 7b), the SDR spectra are strongly shifted toward higher energy. The aspect ratio of the associated model cluster is 3, which corresponds to a contact angle of 67 °, a value which is not too far from the value of 86 ° derived from sessile drop measurements (Table 1). Therefore, the wetting of the second aluminium atomic adlayer deposited on the hydroxylated α-Al_2O_3(0001) compares with the common Al/alumina case with $W_{adh(Al/Al2O3)} < 2\gamma_{Al}$.

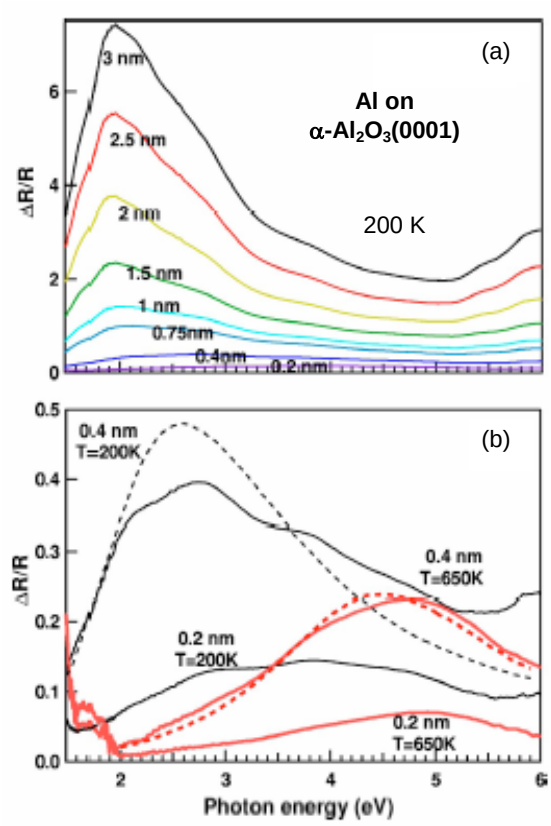

Fig. 7. SDR spectra collected during the deposition of aluminium on α-Al_2O_3(0001): (a) increasing Al average thickness on the substrate at 200 K; (b) 0.2 nm and 0.4 nm thick Al films deposited on the substrate at 200 K and 650 K; model spectra are shown for the two films of 0.4 nm. Note the strong shift in energy between spectra collected at 200K and spectra collected at 600 K (from Ref. 26).

Similar observations are made in the case of the deposition of titanium on α-Al_2O_3(0001). As determined via SDR measurements [8], the aspect ratio of the Ti/alumina particles is ranging between 4 and 8. Therefore, the corresponding wetting angle is between 30° and 50°. The value derived by sessile drop measurements on the Ti/alumina system is higher (78° [19], see Table 1). Several reasons can explain the discrepancy. In the present work, titanium is not at the contact of alumina, but on a titanium oxide film. Moreover, titanium which melting temperature is 2300 K was deposited on a substrate at room temperature, with a supersaturation close to 60, very far from equilibrium conditions. Nevertheless, the main conclusion is here that the titanium does not perfectly wet the alumina substrate, a different conclusion as that drawn during the study of Co/α-Al_2O_3(0001) [5]. In the same way as the Al/alumina system, the Ti/alumina assembly is expected to fail at the interface between the metal and the oxide. Nevertheless, kinetic effects cause the titanium film to spread very well on the alumina surface, leading to an apparent 2D growth mode [29] as analyzed by atomic force microscopy (AFM) (Fig. 8a). At variance, in better agreement with the conclusion that neither silver nor aluminium wet alumina, AFM images of Ag/alumina and Al/alumina show 3D clusters (Figs. 8b and 8c).

Table 1 Estimates of contact angles derived by means of SDR measurements under the assumption that particles are in the form of truncated spheres (see text for discussion). For comparison, values obtained by sessile drop measurements are also given.

	Contact angle for metals on α-Al_2O_3(0001)	
Metal (substrate temperature)	Sessile drop	SDR measurements
Silver (573 K)	127° - 131° [19]	125° [21]
Aluminium (650 K)	86° [19]	67° [26]
Titanium (300 K)	79° [19]	30° - 50° [8]

These experimental findings are consistent with several calculations. Siegel et al. [27] predict a failure at the metal//metal-O-alumina interface when aluminium is deposited on the polar O-terminated α-Al_2O_3(0001) surface. Similar conclusions are drawn by Batirev et al. [30] about the Nb/alumina interface. In the present cases, the very first aluminium and titanium atomic adlayers are seen to react with the surface oxygen atoms of the 'O-terminated' alumina to produce aluminium and titanium oxides, so that everything happens as if the further deposited metallic film was simply at the contact of an oxide. It is assumed that the hydrogen from OH is removed. These results question the idea that the use of polar oxide surfaces can improve the metal/oxide adhesion. It is foreseen that metal/polar oxide adhesion might actually be improved in the case of metals which would undergo some charge transfer while keeping their metallic character.

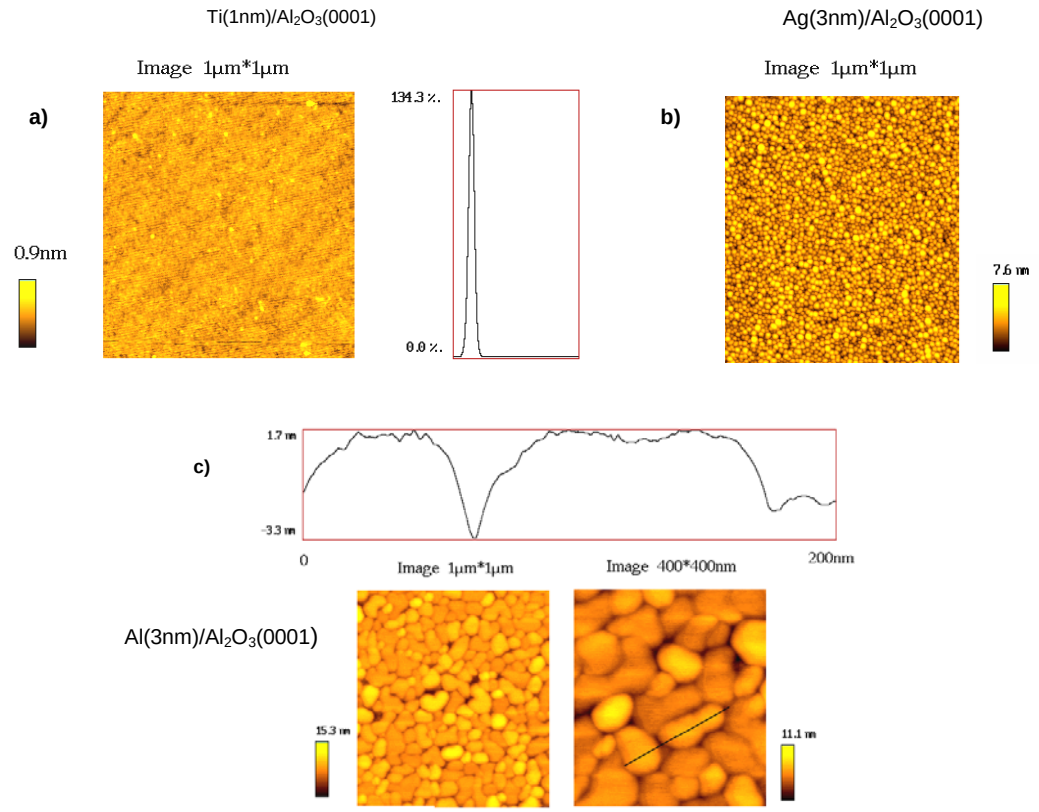

Fig. 8. Atomic force microscopy (AFM) images from titanium silver and aluminium films on α-Al_2O_3(0001) substrates: (a) surface covered by a 1 nm thick film of titanium. The surface shows little roughness while the steps of the bare surface are still visible with a very sharp height distribution. Although titanium is not expected to wet alumina, the observed images are assigned to kinetic effects; (b) surface covered by a 3 nm thick film of silver. Clusters with small aspect ratio are formed (see Fig. 5 and text). The film is far away percolation; (c) surface covered by a 3 nm thick film of aluminium. Flat-top clusters that coalesce are consistent with the formation of clusters with a high aspect ratio (from Refs. 26 and 34).

4. Buffer effect

A very common manner to improve the adhesion at the noble metal/oxide interfaces is the predeposition of a transition-metal buffer [6,31]. For films thick enough to involve dissipation upon failure, adherence energies can be increased by more than one order of magnitude by buffers and reach values higher than 100 $J.m^{-2}$ [31]. As for the mechanism, Elsaesser et al. [32] have predicted that a unique titanium atomic layer can act as a buffer for silver deposited on a MgAl spinel surface so that the electronically depleted transition metal adlayer is expected to 'glue' the silver film. The silver/titanium/α-Al_2O_3(0001) interface appears as a good candidate to examine the buffer effect, since any improvement of the bad Ag/alumina wetting (Fig. 5 and Table 1) should be easily analyzed by SDR. In addition, although titanium does not perfectly wet alumina, kinetics effects result in a good spreading of the titanium film which can thus be assumed to be continuous (Fig. 8c).

4.1 The silver/titanium/α-Al_2O_3(0001) system

The pre-deposition of a 0.1 nm thick titanium film on a α-Al_2O_3(0001) surface hardly improves the wetting by silver, as seen by comparing Figs. 9a and 9b. Therefore, the Ag/Ti/α-Al_2O_3(0001) assembly is not ruled by Elsaesser's model [32]. In fact, the SDR spectrum seen in Fig. 9b is close to that recorded for silver deposited on a thick TiO_2 film (Fig. 9c). The same mechanism as that described for titanium and aluminium depositions applies in the present case. The first layer of titanium is oxidized and, regarding adhesion of a metallic overlayer, it behaves as a common oxide surface.

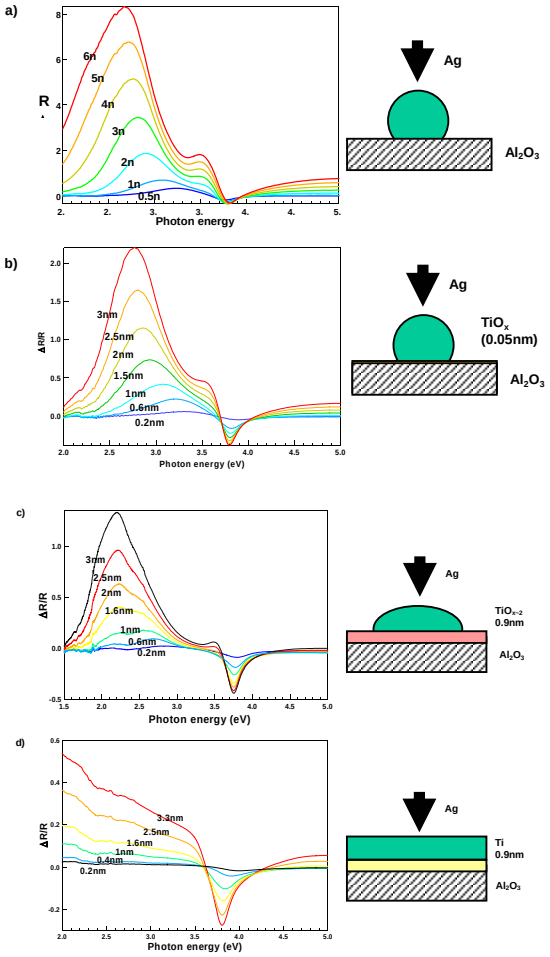

Fig. 9. Wetting of silver on titanium-covered α-Al_2O_3(0001) as analyzed by SDR spectra: (a) bare alumina surface; (b) 0.1 nm thick titanium film; (c) 0.9 nm thick titanium oxidized to give a TiO_2 adlayer; (d) 1 nm thick titanium which, with the exception of the extreme interface, is metallic – In (a), (b) and (c), note the two resonances which are characteristic of particles with small aspect ratio (diameter/height) corresponding to poor wetting; in each figure, the shape of supported particles is schematized in inset (from Ref. 26).

It is only when the predeposited titanium film is thick enough to be metallic that the growth of the silver overlayer undergoes a dramatic change (Fig. 9d). The SDR spectra recorded during the deposition of silver on a 1 nm thick titanium film shows a progressive raise toward the red and a unique resonance which energy tends towards 3.78 eV, the bulk plasmon energy of silver. Both features are characteristic of a continuous silver film [26].

4.2 Wetting of titanium buffers in various chemical states

However, the wetting by silver of the metallic titanium film deposited on alumina dramatically depends on the thickness of that film. The favourable interface orientation of titanium on alumina is Ti(0001)/α-Al_2O_3(0001) with a mismatch of ~ 7%. However, in a first stage, for titanium thickness up to 2 nm, the parameter of the growing titanium film progressively decrease by 4 %, as seen by high energy electron diffraction (RHEED) [33] (Fig. 10a). Between 2 nm and 5 nm, this contracted parameter dominates the diffraction patterns. It was assigned to the formation of ω-Ti [33], a titanium phase usually favoured by high pressure. It is only for titanium films thicker than 6 nm that the RHEED pattern becomes that of the fully relaxed titanium (Fig. 10a). These changes in parameter of the titanium intermediate layer are associated with strong changes in the wetting behaviour of the silver adlayer. In region I, were the parameter is intermediate between alumina and ω-Ti, the silver partially wets the substrate. On ω-Ti, the wetting is very bad, while it becomes excellent on α-Ti, in the limits of the RHEED analysis (Fig. 10b) [33]. Provided the crystallography at the interface of titanium with silver is dictated by the parameters of the ω-Ti and α-Ti phases, such result can be simply explained by the interface mismatch. In the framework of a Ag(111)/Ti(0001) interface, the Ag/Ti mismatch amounts only to -2% for α-Ti while it is much stronger for ω-Ti. Therefore, the behaviour of the Ag/Ti system is consistent with the general idea that, for a given heteroepitaxial system, the adhesion energy decreases when the mismatch increases [18].

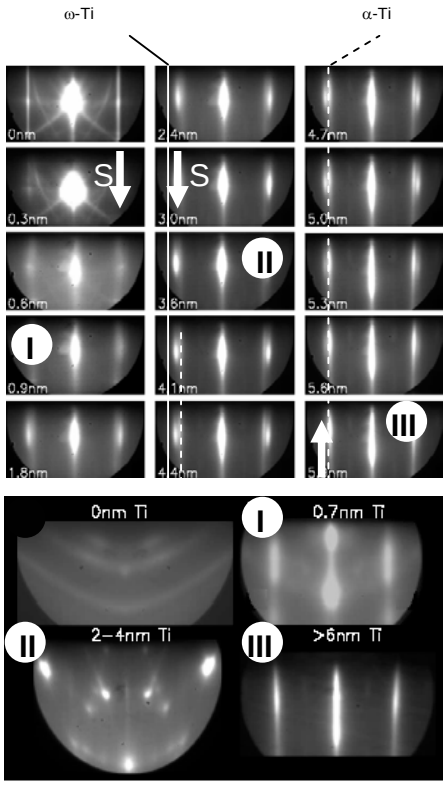

Fig. 10. RHEED analysis of the silver, titanium and alumina assemblies: (a) Ti/α-Al_2O_3(0001) patterns as a function of the titanium coverage; diffraction from the substrate (S), ω-Ti and α-Ti are shown, the former by arrows and the two latter by continuous line and broken line, respectively; (b) Ag/Ti/α-Al_2O_3(0001) patterns corresponding to silver deposition on three different titanium-covered surfaces; surfaces and patterns are shown by numbers I, II, III (from Ref. 33).

5. Conclusion

As a general trend, on thermodynamic grounds, metals poorly wet wide band gap oxides. This has prompted a number of attempts to at least partly control the wetting at these interfaces. Two such approaches have been examined herein in the case of silver, titanium and aluminium on α-Al_2O_3(0001) surfaces, namely the hydroxylation of the alumina surface and the pre-deposition of a transition metal buffer.

The wetting of alumina by titanium and aluminium hardly changes by using hydroxylated alumina surfaces. It is evidenced that the first Al(Ti) atomic adlayer reacts with the surface hydroxyl groups via Al(Ti) + OH to give rise to Al(Ti) oxides. Hydrogen atoms from hydroxyl groups are assumed to be replaced by metal atoms. The then deposited Al(Ti), which remains metallic, is shown to grow in a 3D manner by SDR analysis. Therefore, the Al(Ti)-alumina assembly is expected to fail at the Al(Ti)//Al(Ti)-O-alumina interface, consistently with *ab initio* calculations dealing with Al- and Nb-alumina.

The effect of a titanium buffer on the wetting of silver on alumina is examined as a function of the chemical nature of titanium. As in the case of Al(Ti) deposited on hydroxylated alumina, a very thin oxidized titanium adlayer has no effect on the wetting of the substrate by silver, if one except the trivial fact that the bare alumina surface is replaced by titanium oxide-covered alumina. It is only when the buffer becomes metallic that a dramatic improvement of the wetting by silver is observed. However, the Ag/Ti/alumina wetting is then shown to depend on the crystallography of the titanium film.

The studies presented herein combine analyses of the chemistry and of the wetting at metal/oxide interfaces. Wetting was characterized through in situ analysis of the films during their growth by surface differential reflectance. The method is shown to help to discriminate kinetics and thermodynamics, at least in a qualitative manner.

References

[1] C. T. Campbell, Surf. Sci. Rep. **27**, 1 (1997).
[2] C. R. Henry, Surf. Sci. Reports **31**, 1231 (1998).
[3] J. Jupille, Surf. Rev. Lett. **8**, 69 (2001).
[4] A. Kelber, C. Niu, K. Shepherd, D. R. Jennison, A. Bogicevic, Surf. Sci. **446**, 76 (2000).
[5] S. Chambers, T. Droubay, D. Jennison, T. Mattson, Science **297**, 827 (2002).
[6] G. Dehm, C. Sheu, M. Ruehle, R. Raj, Acta Matter **46**, 759 (1998).
[7] I. Simonsen, R. Lazzari, J. Jupille, S. Roux, Phys. Rev. B **61**, 7722 (2000).
[8] R. Lazzari, I. Simonsen, D. Bedeaux, J. Vlieger, J. Jupille, Europhys. J. B **24**, 267 (2001).
[9] A. M. Stoneham, P. W. Tasker, J. Phys. C: Solid State Phys. **18**, L543 (1985); D. M. Duffy, J. H. Harding, A. M. Stoneham, Acta metall. mater. **40**, S11 (1992).
[10] Y. V. Naidich, Prog. Surface Membrane Sci. **14**, 353 (1981).
[11] F. Didier and J. Jupille, Surf. Sci. **314**, 378 (1994).
[12] R. G. Barrera and C. B. Duke, Phys. Rev. B **13**, 4477 (1976).
[13] R. Sangiorgi, M.L. Muolo, D. Chatain, N. Eustathopoulos, J. Am. Ceram. Soc. **71**, 742 (1988).
[14] F. Didier, J. Jupille, J. Adhesion Sci. Technol. **10**, 373 (1996).
[15] F. Didier, J. Jupille, J. Adhesion 58 (1996).
[16] J. G. Li, Composites Interfaces **1**, 37 (1993).
[17] S. Sounilhac, E. Barthel, F. Creuzet, J. Appl. Phys. **85**, 222 (1999).
[18] P. Müller et R. Kern, Surface Science **457**, 229 (2000).
[19] D. Chatain, L. Coudurier, N. Eustathopoulos, Rev. Phys. Appl. **23**, 1055 (1988).
[20] G. Renaud, R. Lazzari, C. Henry, J. Jupille et al., Science **300**, 1416 (2003).
[21] R. Lazzari, S. Roux, I. Simonsen, J. Jupille, D. Bedeaux, J. Vlieger, Phys. Rev. B **65**, 2354 (2002).
[22] D. Beyssens, C.M. Knobler, Phys. Rev. Lett. **57**, 1433 (1986); J. L. Viovy, D. Beyssens, C. M. Knobler, Phys. Rev. A **37**, 4965 (1988).
[23] C. Revenant, R. Lazzari, G. Renaud, J. Jupille, unpublished results; R. Lazzari, Thesis, Paris (1999).
[24] V. Coustet, J. Jupille, Surf. Sci. 307-309 (1994) 1161 ; Il nuovo Cimento **19**, 1657 (1997).
[25] K. C. Hass, W. F. Schneider, A. Curioni, W. Andreoni, Science **282**, 265 (1998); J. Phys. Chem. B **104**, 5527 (2000).
[26] R. Lazzari, J. Jupille, Phys. Rev. B **71**, 045409 (2005).
[27] D. Siegel, L. Victor, J. Adams, Phys. Rev. B **65**, 085415 (2002).
[28] R. Lazzari, J. Jupille, Surf. Sci. **507-510**, 683 (2002).
[29] E. Bauer, F. van der Merwe, Phys. Rev. B **33**, 3657 (1986).
[30] I. Batirev, A. Alavi, M. Finnis, Faraday Discuss. **114**, 33 (1999).
[31] A. G. Evans, J. W. Hutchinson, Y. Wei, Acta mater. **47**, 4093 (1999).
[32] S. Koestlmeier, C. Elsaesser, Interface Sci. **8**, 41 (2000); J. Phys.: Condens. Matter **12**, 1290 (2000).
[33] E. Sondergard, O. Kerjan, P. Nael, J. Jupille, Surf. Sci. **559**, 131 (2004); E. Sondergard, O. Kerjan, D. Abriou, J. Jupille, Eur. Phys. J. D **24**, 343 (2003).
[34] R. Lazzari, J. Jupille, Surf. Sci. **482**, 823 (2001).

*Corresponding author: jacques.jupille@insp.jussieu.fr, remi.lazzari@insp.jussieu.fr